



Casimir energy for N superconducting cavities: a model for the YBCO (GdBCO) sample to be used in the Archimedes experiment

Annalisa Allocca^{1,2,a}, Saverio Avino^{2,3,b}, Sergio Balestrieri^{1,4,c}, Enrico Calloni^{1,2,d}, Sergio Caprara^{5,6,e}, Massimo Carpinelli^{7,8,f}, Luca D’Onofrio^{1,2,g}, Domenico D’Urso^{7,8,h}, Rosario De Rosa^{7,8,i}, Luciano Errico^{1,2,j}, Gianluca Gagliardi^{2,3,k}, Marco Grilli^{5,6,l}, Valentina Mangano^{5,6,m}, Maria Marsella^{5,6,n}, Luca Naticchioni^{6,o}, Antonio Pasqualetti^{9,p}, Giovanni Piero Pepe^{1,2,q}, Maurizio Perciballi^{6,r}, Luca Pesenti^{7,8,s}, Paola Puppo^{6,t}, Piero Rapagnani^{5,6,u}, Fulvio Ricci^{5,6,v}, Luigi Rosa^{1,2,w}, Carlo Rovelli^{10,11,12,x}, Davide Rozza^{7,8,y}, Paolo Ruggi^{9,z}, Naurang Saini^{5,6,aa}, Valeria Sequino^{1,2,ab}, Valeria Sipala^{7,8,ac}, Daniela Stornaiuolo^{1,2,ad}, Francesco Tafuri^{1,2,ae}, Arturo Tagliacozzo^{1,2,af}, Iara Tosta e Melo^{7,8,ag}, Lucia Trozzo^{2,ah}

¹ Dipartimento di Fisica Ettore Pancini, Università degli Studi di Napoli Federico II, Via Cinthia, Napoli 80126, Italy

² Istituto Nazionale Fisica Nucleare, Sez. Napoli, Via Cinthia, Napoli 80126, Italy

³ Centro Nazionale Ricerche-Istituto Nazionale di Ottica (CNR-INO), Centro Nazionale Ricerche-Istituto Nazionale di Ottica SS Napoli, Via Campi Flegrei, 34, Pozzuoli 80078, Italy

⁴ Centro Nazionale Ricerche, Centro Nazionale Ricerche-Istituto ISASI, Napoli, Via Pietro Castellino, 111, Napoli 80131, Italy

⁵ Dipartimento di Fisica, Università di Roma La Sapienza, Piazzale Aldo Moro, 2, Roma 00185, Italy

⁶ Istituto Nazionale Fisica Nucleare, Sez. Roma 1, Piazzale Aldo Moro, 2, Roma 00185, Italy

⁷ Dipartimento di Scienze Chimiche, Fisiche, Matematiche e Naturali, Università di Sassari, Via Vienna, 2, Sassari 07100, Italy

⁸ Laboratori Nazionali del Sud, Istituto Nazionale Fisica Nucleare, Via Santa Sofia, 62, Catania 95123, Italy

⁹ European Gravitational Observatory - EGO, Via Edoardo Amaldi, Cascina 56021, Italy

¹⁰ Campus of Luminy, Centre de Physique Theorique, Case 907, Marseille 13288, France

¹¹ Aix Marseille Université, CNRS, CPT, UMR 7332, Avenue Robert Schuman, Marseille 13288, France

¹² Université de Toulon, CNRS, CPT, UMR 7332, Avenue de L’Université, La Garde 83130, France

Received: 20 March 2022 / Accepted: 30 June 2022

© The Author(s) 2022

Abstract In this paper we study the Casimir energy of a sample made by N cavities, with $N \gg 1$, across the transition from the metallic to the superconducting phase of the constituting plates. After having characterised the energy for the configuration in which the layers constituting the cavities are made by dielectric and for the configuration in which the layers are made by plasma sheets, we concentrate our analysis on the latter. It represents the final step towards the macroscopical characterisation of a “multi-cavity” (with N large) necessary to fully understand the behaviour of the Casimir energy of a YBCO (or a GdBCO) sample across the transition. Our analysis is especially useful to the Archimedes experiment, aimed at measuring the interaction of the electromagnetic vacuum energy with a gravitational field. To this purpose, we aim at modulating the Casimir energy of a layered structure, the multi-cavity, by inducing a transition from the metallic to the superconducting phase. After having characterised the Casimir energy of such a structure for both the metallic and the superconducting phase, we give an estimate of the modulation of the energy across the transition.

^a e-mail: annalisa.allocca@na.infn.it

^b e-mail: saverio.avino@ino.cnr.it

^c e-mail: sergiobale2@gmail.com

^d e-mail: enrico.calloni@na.infn.it

^e e-mail: sergio.caprara@roma1.infn.it

^f e-mail: mcarpinelli@uniss.it

^g e-mail: ldonofrio@na.infn.it

^h e-mail: ddurso@uniss.it

ⁱ e-mail: rosario.derosa@na.infn.it

^j e-mail: luciano.errico@na.infn.it

^k e-mail: gianluca.gagliardi@ino.it

^l e-mail: marco.grilli@roma1.infn.it

^m e-mail: valentina.mangano@roma1.infn.it

ⁿ e-mail: maria.marsella@roma1.infn.it

^o e-mail: luca.naticchioni@roma1.infn.it

1 Introduction

The principal goal of the Archimedes experiment [1] is to measure the coupling of the vacuum fluctuations of Quantum Electrodynamics (QED) to the gravitational field of the Earth. The coupling is obtained, as usual in Quantum Field Theory in Curved spacetime [2–5], assuming the Einstein tensor to be proportional to the expectation value of the regularized and renormalized energy-momentum tensor of matter fields, in particular, for the Archimedes experiment, of the electromagnetic field. The idea is to weigh the vacuum energy stored in a rigid Casimir cavity [6], made by parallel conducting plates, by modulating the reflectivity of the plates upon inducing a transition from the metallic to the superconducting state [1]. The “modulation factor” is defined as $\eta = \frac{\Delta E}{E_0}$ where $\frac{\Delta E}{A}$ is the difference of Casimir energy (per square meter) in the normal and in the superconducting state, and $\frac{E_0}{A}$ is the (absolute value) of the Casimir energy (per square meter), at zero temperature, of an ideal cavity of the same thickness d : $\frac{E_0}{A} = \frac{\pi^2 \hbar c}{720d^3}$.

In Ref. [1] it was shown that, in order to measure such an effect, η must be of the order $\eta \sim 10^{-5}$ and that, to this purpose, a multi-cavity, obtained by superimposing many cavities must be used. This structure is natural in the case of crystals of type-II superconductors, particularly cuprates, being composed by Cu–O planes, that undergo the superconducting transition, separated by nonconducting planes. A crucial aspect to be tested is the behavior of the Casimir energy [6] for a multi-cavity when the layers undergo the phase transition from the metallic to the superconducting phase. In a previous paper [7] a careful study for such a type of structure has been carried out for a sample made by up to three “relatively thick” (of the order of ten nanometer) dielectric layers. In the present paper we extend the analysis to any number of cavities for both situations: layers consisting of “thick” dielectric slabs and layers consisting of “thin” plasma sheets.

Indeed, in Ref. [8], considering a cavity based on a high- T_c layered superconductor, a factor as high as $\eta = 4 \times 10^{-4}$ has been estimated (for flat plasma sheets at zero temperature and no conduction in the normal state, so that ΔE corresponds to the energy of the ideal cavity, and charge density $n = 10^{14} \text{ cm}^{-2}$). The Archimedes sensitivity is expected to be capable of assessing the interaction of gravity and vacuum energy also for values lower than $\eta = 4 \times 10^{-4}$, up to 1/100 of this value [1]. It is then crucial to understand the level of modulation achievable with layered superconducting structures. This is the scope of the present paper.

Considering in particular the multi-cavity, the general assumption adopted so far has been that the Casimir energy obtained by overlapping many cavities is the sum of the energies of each individual cavity. This is true if the *distances* between neighboring cavities are large (in the sense that the thickness of each metallic layer separating the various cavities is very large with respect to the penetration depth of the radiation field). Of course, this is no longer true if the thickness of these metallic inter-cavity layers gets thinner and thinner.

Section II studies the Casimir energy of a multilayered cavity, assuming either dielectric or plasma sheet matching conditions at each interface between the layers. In Sec. III, numerical calculations are carried out and an analytic model capable of describing the Casimir energy at finite temperature is given. Finally, in Sec. IV, a possible model for describing the variation (and the modulation) of the Casimir energy across the transition is introduced. Our concluding remarks are found in Sec. V.

^P e-mail: antonio.pasqualetti@ego-gw.it

^Q e-mail: gpepe@na.infn.it

^R e-mail: maurizio.perciballi@roma1.infn.it

^S e-mail: lpesenti@uniss.it

^T e-mail: paola.puppo@roma1.infn.it

^U e-mail: piero.rapagnani@roma1.infn.it

^V e-mail: fulvio.ricci@roma1.infn.it

^W e-mail: luigi.rosa@na.infn.it (corresponding author)

^X e-mail: rovelli.carlo@gmail.com

^Y e-mail: davide.rozza@lns.infn.it

^Z e-mail: paolo.ruggi@ego-gw.it

^{aa} e-mail: Naurang.Saini@roma1.infn.it

^{ab} e-mail: valeria.sequino@na.infn.it

^{ac} e-mail: vsipala@uniss.it

^{ad} e-mail: daniela.stornaiuolo@unina.it

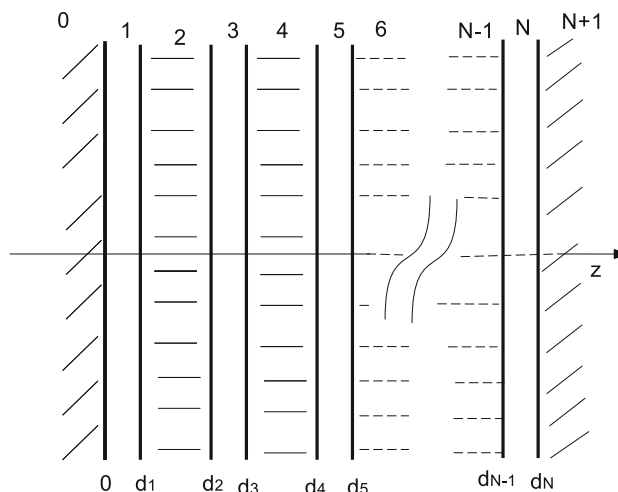
^{ae} e-mail: francesco.tafari@na.infn.it

^{af} e-mail: arturo.tagliacozzo@na.infn.it

^{ag} e-mail: itostaemelo@uniss.it

^{ah} e-mail: lucia.trozzo@na.infn.it

Fig. 1 The layered structure considered in this paper. For the dielectric case all even-numbered regions include a dielectric material and all odd-numbered regions include vacuum. For plasma-sheet model the layers marked by bold lines are simple interfaces of zero thickness and d_i is the thickness of the i -th slab



2 The Casimir energy of N coupled cavities

In this section we deduce the Casimir Energy of n coupled cavities, even though in the present paper we are interested in applying our results to plasma sheets, we will discuss the case of dielectrics first and then recover the plasma sheets results as a suitable limiting case.

In the following, referring to Fig. 1, d_i is the distance of the i -th cavity from the $(i - 1)$ -th, (thickness of the i -th cavity), within the slabs 1, 3, 5 and N there is vacuum while within the regions 0, 2, 4, 6 and $N + 1$ there is dielectric (in the case of dielectric model) or vacuum (for the plasma-sheet model). The thickness of the regions 0 and $N + 1$ is assumed to be infinite.

The general expression for the Casimir energy (per unit area), at finite temperature, will be written in the usual manner [9–11]

$$E = k_B T \sum_{l=0}^{\infty} \int \frac{d\mathbf{k}_{\perp}}{(2\pi)^2} [\log \Delta^{\text{TE}}(\zeta_l) + \log \Delta^{\text{TM}}(\zeta_l)] \tag{1}$$

where the Δ are the so called generating functions (in the following we will omit the subscript $\text{TM}(\text{TE})$ if no ambiguity is generated), $\zeta_l = 2\pi l k_B T$ are the Matsubara frequencies, k_B is the Boltzmann constant, $l = 0, 1, 2, \dots$, and the superscript $'$ on the sum means that the zero mode must be multiplied by a factor $\frac{1}{2}$. The generating functions are obtained by computing the determinant of the most general boundary conditions at each singular layer located at $d_0, d_0 + d_1, d_0 + d_1 + d_2 \dots$ etc. (see Fig. 1; see also the appendix [12]).

For the sake of clarity, we only give here the general argument about the procedure for obtaining the generating functions, referring the reader to the appendix for the complete computation. In the appendix we show that the Δ functions can be written in terms of a sort of generalised reflection coefficients:

$$\begin{aligned} R_{\text{TM}}^{i,j} &= \frac{\epsilon_j(i\zeta_l)K_i - \epsilon_i(i\zeta_l)K_j - 2\frac{\Omega}{\zeta_l^2}K_iK_j}{\epsilon_j(i\zeta_l)K_i + \epsilon_i(i\zeta_l)K_j + 2\frac{\Omega}{\zeta_l^2}K_iK_j}, & R_{\text{TE}}^{i,j} &= \frac{K_i - K_j + 2\Omega}{K_i + K_j + 2\Omega}, \\ S_{\text{TM}}^{i,j} &= \frac{\epsilon_j(i\zeta_l)K_i - \epsilon_i(i\zeta_l)K_j + 2\frac{\Omega}{\zeta_l^2}K_iK_j}{\epsilon_j(i\zeta_l)K_i + \epsilon_i(i\zeta_l)K_j + 2\frac{\Omega}{\zeta_l^2}K_iK_j}, & S_{\text{TE}}^{i,j} &= \frac{K_i - K_j - 2\Omega}{K_i + K_j + 2\Omega}, \\ T_{\text{TM}}^{i,j} &= \frac{\epsilon_j(i\zeta_l)K_i + \epsilon_i(i\zeta_l)K_j - 2\frac{\Omega}{\zeta_l^2}K_iK_j}{\epsilon_j(i\zeta_l)K_i + \epsilon_i(i\zeta_l)K_j + 2\frac{\Omega}{\zeta_l^2}K_iK_j}, & T_{\text{TE}}^{i,j} &= \frac{K_i + K_j - 2\Omega}{K_i + K_j + 2\Omega}, \end{aligned}$$

where $K_i = \sqrt{k_{\perp}^2 + \epsilon_i(i\zeta_l)\zeta_l^2}$, $k_{\perp} = (k_x, k_y)$, $\Omega = \frac{\mu_0 n_{2D} q^{*2}}{m^*}$, μ_0 is the magnetic permeability of vacuum, n_{2D} is the two dimensional carrier density in the layer, and q^* and m^* , respectively, their charge and mass. The standard dielectric boundary conditions (dbc) will be recovered by imposing $\Omega = 0$ and the plasma sheet boundary conditions (psbc) by requiring $\epsilon_i(i\zeta_l) = 1, \forall i$ (in this case, $K_i = K_j$).

After introducing the auxiliary functions

$$\begin{aligned} E^{ijk} &= e^{-2d_j K_j} S^{j,k} R^{i,j} + 1, \\ F^{ijk} &= e^{-2d_j K_j} R^{i,j} T^{j,k} + R^{j,k}, \end{aligned}$$

$$G^{ijk} = e^{-2d_j K_j} S^{j,k} T^{i,j} + S^{i,j},$$

$$H^{ijk} = S^{i,j} R^{j,k} + e^{-2d_j K_j} T^{i,j} T^{j,k}$$

and (henceforth, we will assume all the cavities to be equal and consider only the indices $\{ijk\} = \{012\}$), on defining:

$$I_1 = E^{012}; \quad I_2 = F^{012} e^{-2d_2 K_2} G^{012},$$

$$I_n = F^{012} e^{-2d_2 K_2} \left(H^{012} e^{-2d_2 K_2} \right)^{n-2} G^{012}, \quad \text{for } n \geq 3,$$

we can proceed to compute the generating functions.

2.1 The dielectric case

Let us consider Casimir cavities made of dielectric layers (of thickness d_i). To obtain the general expression for the Δ functions we can proceed inductively (a very detailed discussion up to three cavities can be found in Ref. [7]). For the cavity characterised by the numbers (012) in Fig. 1, with $\epsilon_0 = \epsilon_2$, the generating function, for TM and TE modes, respectively, is obtained in the usual manner [7, 10] (see appendix). After regularization, i.e., setting to zero the Casimir energy when the two cavities are infinitely far away, the result can be written as $\Delta_1 = E^{012} = I_1$. Let us now consider two cavities [(012), (234) in Fig. 1]. In this case, the generating function is the determinant of the 8×8 matrix made by the first rows and columns of the matrix given in the appendix [7]. It can be written as a 2×2 block matrix, thus [17, 18]

$$\Delta = \det \begin{pmatrix} A & B \\ C & D \end{pmatrix} = \det(A) \det(1 - A^{-1} B D^{-1} C) \det(D),$$

where $\{A, B, C, D\}$ are 4×4 matrices, with $\det(A) = \det(D) = \Delta_1$.

When the two cavities are infinitely far away from each other ($d_2 \rightarrow \infty$), $C = 0$, $\Delta = \det(A) \det(D) =: \Delta_2$ and the Casimir energy will be simply the sum of the energies of the two cavities, $\log(\Delta_2) = \log(\Delta_1^2) = 2 \log(\Delta_1)$. When they are brought at a distance d_2 from each other, in addition to the previous energy, there is the interaction energy accounted for by the term $\det(1 - A^{-1} B D^{-1} C)$. In this case $\Delta_2 = \det(A) \det(D) \det(1 - A^{-1} B D^{-1} C)$ and, after regularization, it can be written (see appendix) as $\Delta_2 =: I_1^2 + I_2$, which defines I_1 and I_2 , so that the corresponding Casimir energy depends on $\log \Delta_2 = \log(I_1^2 + I_2) = \log(I_1^2) + \log(1 + I_2/I_1^2)$. The first term is simply the sum of the energies of the two cavities taken independently, the second term is the interaction energy between the two [7]. Therefore we can always reduce ourselves to the computation of determinants of products of 4×4 matrix. The interaction in the case of $n \geq 3$ cavities is accounted for by the term I_n .

In this manner, using the inductive principle, it is not difficult to convince oneself that the generic Δ_N functions for the case of N dielectric cavities can be obtained in the following manner (a sort of Feynman diagram for the generating functions): let us define $\{k_1, k_2, \dots, k_J\}$ to be the J -th integer partition of N and Q_J its multiplicity (the number of combinations that contain the same type of I_k but in a different position) then

$$\Delta_N = \sum_J Q_J (I_{k_1} I_{k_2} \dots I_{k_J}).$$

So, for example,

$$\begin{aligned} \Delta_1 &= I_1, \\ \Delta_2 &= (I_1)^2 + I_2, \\ \Delta_3 &= (I_1)^3 + I_1 I_2 + I_2 I_1 + I_3 = (I_1)^3 + 2I_1 I_2 + I_3, \\ \Delta_4 &= I_4 + I_1 I_3 + I_3 I_1 + I_2^2 + I_1 I_1 I_2 + I_1 I_2 I_1 + I_2 I_1 I_1 + I_1^4 \\ &= I_4 + 2I_1 I_3 + I_2^2 + 3I_1^2 I_2 + I_1^4, \end{aligned}$$

and, e.g.,

$$\begin{aligned} \Delta_{10} &= I_1^{10} + 9I_1^8 I_2 + 28I_1^6 I_2^2 + 35I_1^4 I_2^3 + 15I_1^2 I_2^4 + I_2^5 + 8I_1^7 I_3 + 42I_1^5 I_2 I_3 + 60I_1^3 I_2^2 I_3 \\ &+ 20I_1 I_2^3 I_3 + 15I_1^4 I_3^2 + 30I_1^2 I_2 I_3^2 + 6I_2^2 I_3^2 + 4I_1 I_3^3 + 7I_1^6 I_4 + 30I_1^4 I_2 I_4 + 30I_1^2 I_2^2 I_4 \\ &+ 4I_2^3 I_4 + 20I_1^3 I_3 I_4 + 24I_1 I_2 I_3 I_4 + 3I_3^2 I_4 + 6I_1^2 I_4^2 + 3I_2 I_4^2 + 6I_1^5 I_5 + 20I_1^3 I_2 I_5 \\ &+ 12I_1 I_2^2 I_5 + 12I_1^2 I_3 I_5 + 6I_2 I_3 I_5 + 6I_1 I_4 I_5 + I_5^2 + 5I_1^4 I_6 + 12I_1^2 I_2 I_6 + 3I_2^2 I_6 \\ &+ 6I_1 I_3 I_6 + 2I_4 I_6 + 4I_1^3 I_7 + 6I_1 I_2 I_7 + 2I_3 I_7 + 3I_1^2 I_8 + 2I_2 I_8 + 2I_1 I_9 + I_{10}. \end{aligned}$$

for ten cavities.

Table 1 The ratio $\frac{E[N]}{NE[1]}$ as a function of the number of cavities

N	$\frac{1}{N} \frac{E[N]}{E[1]}$
1	1.0000
2	1.0125
3	1.0181
4	1.0212
5	1.0232
6	1.0246
7	1.0256
8	1.0263
9	1.0269
10	1.0274
11	1.0278
13	1.0284
15	1.0288
17	1.0292
19	1.0294

2.2 The plasma sheets case

These formulae can be extended to the case in which the layers are characterised as plasma sheets. For example, the two dielectric cavities (012) and (234) can describe three plasma-sheet cavities, (012), (123), (234), by imposing $\epsilon_i = 1$, and $\Omega \neq 0$. In other words, two dielectric cavities needs four layers located at $0, d_1, d_1 + d_2, d_1 + d_2 + d_3$ but the same four layers correspond to three cavities having plasma sheet as boundaries. Consequently N_{ps} (odd) plasma sheets can be obtained by $n = \frac{N_{ps}+1}{2}$ standard dielectrics by simply imposing $\epsilon_i(i\zeta) = 1$, and the extension of the previous formulae to the case of an odd number of plasma sheets is straightforward.

The case of an even number of plasma sheets is more involved. It can be obtained starting with $N_{ps} + 1$ (N_{ps} even) cavities and moving the last layer to infinity. From the mathematical point of view, this procedure corresponds to introducing a term I'_n (which describes the interaction of the last interface with all the others), defined like as

$$I'_1 = 1; \quad I'_n = \lim_{G \rightarrow G'} I_n, \quad \text{if } n \geq 2; \quad \text{having defined } G'^{ijk} := S^{ij}. \tag{2}$$

In this manner, we have for two and four plasma sheet (please note that it is necessary to perform the limiting procedure first and then to group together the various terms)

$$\begin{aligned} \Delta_2^{ps} &= \lim_{G \rightarrow G'} \Delta_{2+1}^{ps} = \lim_{G \rightarrow G'} \Delta_2 = \lim_{G \rightarrow G'} [(I_1)^2 + I_2] = I_1 I'_1 + I'_2 = I_1 + I'_2; \\ \Delta_4^{ps} &= \lim_{G \rightarrow G'} \Delta_{4+1}^{ps} = \lim_{G \rightarrow G'} \Delta_3 = \lim_{G \rightarrow G'} [(I_1)^3 + I_1 I_2 + I_2 I_1 + I_3] \\ &= I_1 I_1 I'_1 + I_1 I'_2 + I_2 I'_1 + I'_3 = I_1^2 + I_2 + I_1 I'_2 + I'_3. \end{aligned} \tag{3}$$

The fact that only one term at a time takes the prime corresponds to the fact that the last cavity only must be sent to infinity (i.e. $d_N \rightarrow \infty$ while leaving all the remaining $d_i, i \neq N$ finite).

3 Numerical results

We are now in the position to discuss the dependence of the Casimir Energy of a N -cavity made of N -plasma sheets. We underline the fact that the contribution of TE modes results various order of magnitude less than the one from TM modes. For this reason, in the following, it will be simply omitted.

We start by considering the variation of the Casimir energy as a function of the number of cavities for fixed thickness $d_i = 2$ nm and $\Omega = \frac{\mu_0 n^2 D q^{*2}}{m^*} = 49593.3 \text{ m}^{-1}$ (see Refs. [16, 19]). We get $\frac{E[1]}{A} = -0.000197 \text{ Jm}^{-2}$ and, for the ratio $\frac{E[N]}{NE[1]}$ between the Casimir Energy of N cavities $E[N]$, and the product $NE[1]$ between the number of cavities and the energy of a single cavity $E[1]$, we find the values quoted in the following Table 1.

The best fit is given by

$$\frac{1}{N} \frac{E[N]}{E[1]} = 1.034 - \frac{0.034}{N^{0.71}}, \tag{5}$$

Fig. 2 The exact numerical result (dots) and the fitted results given by Eq. (5) (green line) of the function $E[N]/(NE[1])$ for $d = 2$ nm

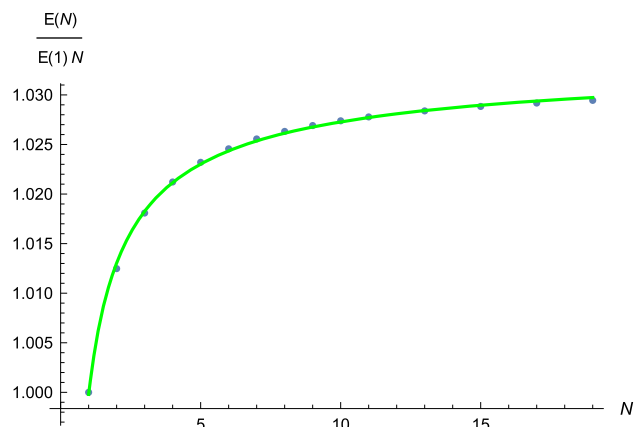
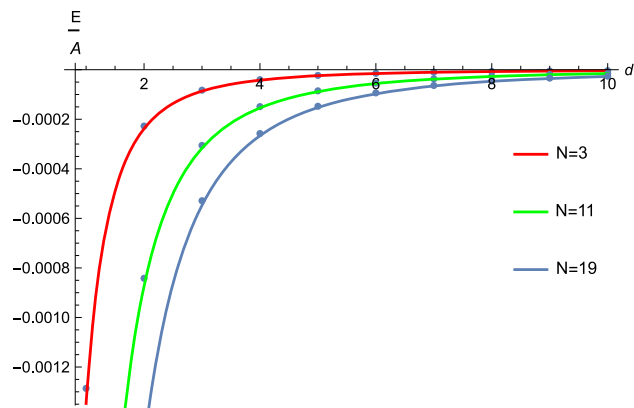


Fig. 3 A comparison between exact numerical values of the Casimir energy (dots) and the approximated formula, Eq. (7) (lines), with d expressed in nm and E/A in J/m^2



that gives a clear indication of the presence of an asymptote for $N \rightarrow \infty$. In Fig. 2 a comparison between the exact numerical result and the analytical fitted behaviour up to $N = 19$ [Eq. (5)] is shown.

Thus, we obtained an asymptotic expression for the Casimir energy for large N ,

$$E[N] \simeq (1.034 E[1])N \tag{6}$$

and deduced that the coupling of the various cavities resulted in an increase of the Casimir energy of 3.4%. This result is very different from the result for dielectric layers, in which a strong coupling between the two and the three nearest cavities is found (see [7]). Indeed, considering (for giving an idea) a cavity made by two dielectric slabs (for example made by Niobium) 2 nm thick and separated by 2 nm of vacuum, we find $\frac{E[2]-2E[1]}{E[2]} \simeq 30\%$ to be compared with the 1.2% obtained for plasma-sheet.

Needless to say this result depends on the thickness of the cavity. For example in the same situation but with (more realistic) thickness of the dielectric cavities (and of the vacuum) $d = 50$ nm, the same ratio turns out to be $\simeq 3\%$. The same behaviour is found for the case of three cavities, see discussion in [7] sec. 5.

In order to have further confirmation of eq.(6), which is, after all, obtained at fixed Ω and d , we can use the Casimir energy functional dependence of a single cavity on these two parameters as reported in [15]: $E[1] = 5 \times 10^{-3} \hbar c \sqrt{\frac{\Omega}{d^5}}$. With this in mind, we assume for $E[N]/A$ the following functional form $E[N]/A = -(1.034 N)K \hbar c \frac{\Omega^\alpha}{d^\beta}$, with arbitrary K , α and β , and find their best estimate, using the method of least-squares, with respect to the exact results obtained numerically. We found $K = 5.0 \times 10^{-3}$, $\beta = 2.4998$ and $\alpha = 0.4998$, in perfect agreement with Ref. [15]. The comparison, shown in Fig. 3 (Casimir energy as a function of d) and Fig. 4 (Casimir energy as a function of Ω), are a clear indication of the validity of the expression (6).

In conclusion, a good approximation for the Casimir Energy (at fixed temperature) for N plasma-sheet cavities can be written as

$$\frac{E[N]}{A} = -\left(1.034 K \hbar c \frac{\sqrt{\Omega}}{d^{5/2}}\right)N = (-1.63 \times 10^{-28} \text{ (Jm)}) \left(N \frac{\sqrt{\Omega}}{d^{5/2}} \text{ (m}^{-3}\text{)}\right) \tag{7}$$

with $E[N]/A$ measured in Jm^{-2} .

Based on the above formulae, in the following section we give an estimate for the variation of the Casimir energy across the metal-superconductor transition.

Fig. 4 A comparison between exact values of the Casimir energy (dots) and the approximated formula (lines), for $d = 2$ nm, with Ω expressed in nm^{-1} E/A in J/m^2

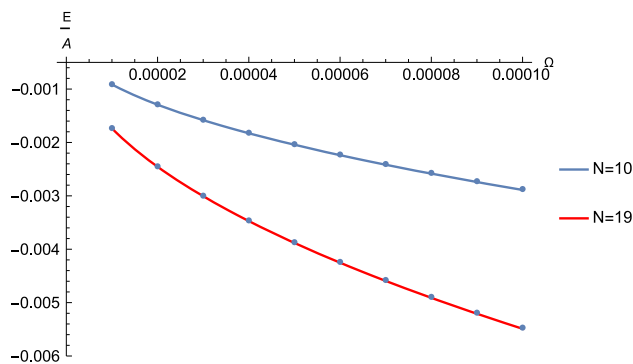
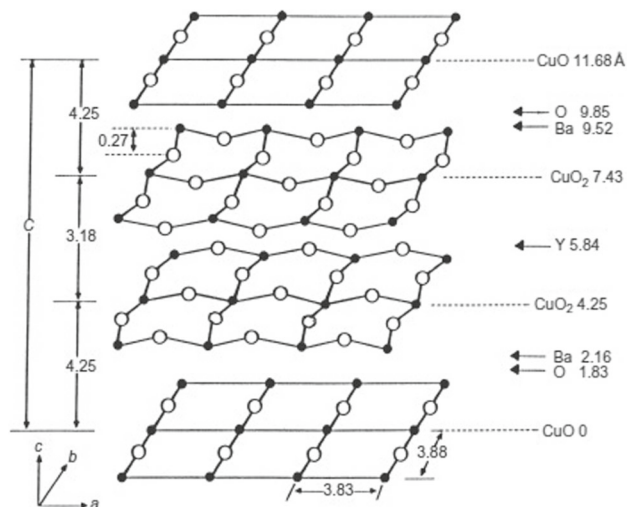


Fig. 5 Typical layered structure of $\text{YBa}_2\text{Cu}_3\text{O}_7$ [22]



4 The variation of the Casimir energy in the YBCO

The typical structure of a YBCO cell (a very well studied material for its numerous fundamental applications [20, 21]) is represented in Fig. 5, in which $\delta = 4.25\text{\AA}$ is the thickness of our plasma sheet and $d = 3.18\text{\AA}$ is the distance between the layers.

By observing that [16] $\Omega(0) = \frac{\delta}{2\lambda_{ab}^2(0)}$, at $T = 0$ K, we can write for the Casimir energy of one cavity in the superconducting state as

$$\frac{E(0)}{A} = -1.63 \times 10^{-28} \sqrt{\frac{\delta}{2d^5}} \frac{1}{\lambda_{ab}(0)} \tag{8}$$

Using the BCS relation $\lambda(T) = \frac{\lambda(0)}{\sqrt{1-(T/T_c)^{4/3}}}$ [22], corresponding to the case of d -wave pairing, as it is suitable for cuprates, for $T < T_c$ and for one cavity we get

$$\frac{E(T)}{A} = - \frac{1.63 \times 10^{-28}}{\lambda_{ab}(T)} \sqrt{\frac{\delta}{2d^5}} = -1.63 \times 10^{-28} \sqrt{\frac{\delta}{2d^5}} \frac{\sqrt{1-(T/T_c)^{4/3}}}{\lambda_{ab}(0)} \tag{9}$$

Thus, using for $\text{YBa}_2\text{Cu}_3\text{O}_7$ [19], $T_c = 92$ K, $\lambda_{ab}(0) = 1415$ \AA , $d = 3.36$ \AA , and $\delta = 5.84$ \AA , we have

$$\frac{E(90)}{A} = -9.51 \times 10^{-3} \sqrt{1-(90/92)^{4/3}} = -0.001616 \text{ Jm}^{-2}. \tag{10}$$

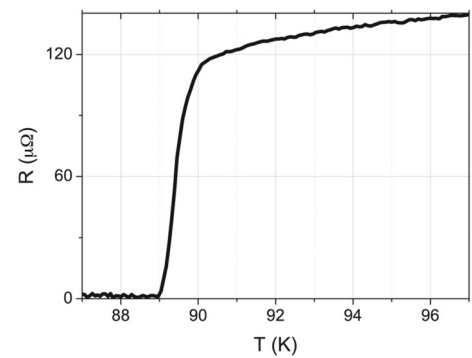
For the normal phase, $T > T_c$, we will use the data (and formulae) of Ref. [23].

At $T = 100$ K, we have $n_{3D} = 3.1 \times 10^{25} \text{ m}^{-3}$, which implies $n_{2D} = n_{3D} \delta = (3.1 \times 10^{25})(5.84 \times 10^{-10}) = 1.810 \times 10^{16} \text{ m}^{-2}$. In the Archimedes experiment a transition of a few degrees around the critical temperature is required to induce a continuous superconducting-normal transition. For this reason, in the following, we will choose, to fix the ideas, a four degree interval around T_c , thus for $T = 94$ K, we have $n_{2D} = 1.317 \times 10^{16} \frac{94}{100} = 1.702 \times 10^{16} \text{ m}^{-2}$. Consequently, $\Omega = \frac{\mu_0 n_{2D} e^2}{2m^*} = 300.505 \text{ m}^{-1}$, and

$$\frac{E(94)}{A} = -1.63 \times 10^{-28} \sqrt{\frac{\Omega}{d^5}} = -0.001365 \text{ Jm}^{-2}.$$

Thus,

Fig. 6 The transition of the sample of YBCO we are using



$$\frac{\Delta E}{A} = \frac{E(94) - E(90)}{A} = 0.000251 \text{ Jm}^{-2}.$$

As revealed by an inspection of the table in Ref. [19], it is clear that the previous results depend in a crucial way on the sample of YBCO used. A typical Resistance vs. Temperature curve of the YBCO crystals we are planning to use in the Archimedes experiment is reported in Fig. 6. Our reference values are $T_c = 89 \text{ K}$ and $\lambda_{ab}(0) = 1030 \text{ \AA}$ [24], thus, assuming all the other parameters unaltered, we have $\frac{E(87)}{A} = -0.002258 \text{ Jm}^{-2}$ and, in the normal phase, $T = 91 \text{ K}$, $\frac{E(91)}{A} = -0.001343 \text{ Jm}^{-2}$ so that $\frac{\Delta E}{A} = \frac{E(91) - E(87)}{A} = 0.0009142 \text{ Jm}^{-2}$.

5 Conclusions

We have proposed a model for computing the variation of the Casimir energy of a YBCO sample across the metal-superconductor transition.

We have constructed a powerful procedure to compute the renormalised Casimir energy both in the case of cavities made of a large number of thick dielectric layers and in the case of cavities made by a large number of thin plasma sheet layers.

Our main assumption is that the last case can be used to describe the Casimir energy in YBCO and, more generally in cuprates (GdBCO), because of their natural built-in layered structure, both in the normal and in the superconducting phase. While the approach used here rests on a marked microscopic layer structure of the superconductor, the model uses phenomenological macroscopic parameters assuming which include mediated properties of the layer structure itself. The analysis conducted in [16] of the correlation between Casimir energy and experimental parameters such as penetration length in the plane λ_{ab} , effective mass m^* and critical temperature T_c is rather reassuring. Indeed, after their phenomenological analysis, the authors explicitly state in the conclusions that the plasma sheet model provides a good description for the behaviour of copper oxide HTSCs superconductors.

We suggested a possible way of characterising the variation of the Casimir energy at the metal-superconductor transition, giving a numerical estimate for the specific YBCO sample that we are using in the Archimedes experiment (at this time both YBCO and GdBCO superconductors are under consideration).

The computed value for the “modulation factor” $\eta = \frac{\Delta E}{E_0}$, for one cavity (since the total number of cavities within a sample will depend on the ratio between its total thickness and the thickness of the single layer, it is better to use the modulation factor referred to one cavity only), is thus in the range $\left(\frac{0.00025}{0.27} \sim\right) 0.0009 \leq \frac{\Delta E}{E_0} \leq 0.003 \left(\sim \frac{0.0009}{0.27}\right)$ (E_0/A being the energy (per square meter) of an ideal cavity 11.68 \AA thick) see Fig. 5, which is quite reassuring for the Archimedes experiment [1]. Of course, although encouraging, these results must be considered as an estimate of the orders of magnitude involved that reinforces the hypothesis that the variation of Casimir energy is not negligible compared to the condensation energy in a type II superconductor.

Acknowledgements D. D’Urso and D. Rozza acknowledge Università degli Studi di Sassari with “Fondo di Ateneo per la ricerca 2019” and “Fondo di Ateneo per la ricerca 2020”.

Funding Open access funding provided by Università degli Studi di Napoli Federico II within the CRUI-CARE Agreement.

Data Availability Statement No datasets were generated or analysed during the current study.

Open Access This article is licensed under a Creative Commons Attribution 4.0 International License, which permits use, sharing, adaptation, distribution and reproduction in any medium or format, as long as you give appropriate credit to the original author(s) and the source, provide a link to the Creative Commons licence, and indicate if changes were made. The images or other third party material in this article are included in the article’s Creative Commons licence, unless indicated otherwise in a credit line to the material. If material is not included in the article’s Creative Commons licence and your intended

use is not permitted by statutory regulation or exceeds the permitted use, you will need to obtain permission directly from the copyright holder. To view a copy of this licence, visit <http://creativecommons.org/licenses/by/4.0/>.

Appendix A

The generating functions are obtained by imposing the most general boundary conditions at each singular layer located at $d_0, d_0 + d_1, d_0 + d_1 + d_2 \dots$ etc. (see Fig. 1). These are obtained, as usual, by integrating the Maxwell equations

$$\begin{aligned} \nabla \cdot \mathbf{D} &= \rho, & \nabla \times \mathbf{E} + \frac{\partial \mathbf{B}}{\partial t} &= 0, \\ \nabla \cdot \mathbf{B} &= 0, & \nabla \times \mathbf{H} - \frac{\partial \mathbf{D}}{\partial t} &= \mathbf{J}, \\ \mathbf{D} &= \epsilon \mathbf{E}, & \mathbf{B} &= \mu \mathbf{H}, \quad (\epsilon = \epsilon_0, \mu = \mu_0 \text{ in vacuum}), \end{aligned}$$

across the discontinuity layers [12],

$$\begin{aligned} (\mathbf{D}_i - \mathbf{D}_{i-1}) \cdot \mathbf{n} &= \sigma, & (\mathbf{B}_i - \mathbf{B}_{i-1}) \cdot \mathbf{n} &= 0, \\ \mathbf{n} \times (\mathbf{E}_i - \mathbf{E}_{i-1}) &= 0, & \mathbf{n} \times (\mathbf{H}_i - \mathbf{H}_{i-1}) &= \mathbf{J}, \end{aligned}$$

where $\mathbf{n} = \hat{z}$ is the normal to the layers (parallel to the z -axis, going from the i -th to the $i + 1$ -th layer), σ is the surface charge density, and \mathbf{J} is the surface current density respectively (in principle they could be different at each layer, but we will not consider this situation). By virtue of the translational invariance in the (x, y) plane we can set

$$\mathbf{E} = \mathbf{f}(z)e^{i(k_{\parallel} \cdot \mathbf{x}_{\parallel} - \omega t)}, \quad \mathbf{B} = \mathbf{g}(z)e^{i(k_{\parallel} \cdot \mathbf{x}_{\parallel} - \omega t)}.$$

In the following, when discussing the plasma sheet model, we will consider the so called hydrodynamic model [13, 14], in which a continuous fluid with mass m^* and charge q^* is uniformly distributed in the layer with an overall-neutralizing background charge. The fluid displacement ξ is purely tangential, $\xi \equiv (\xi_x, \xi_y)$ with surface charge and current densities related to the tangential component of the electric field \mathbf{E}_{\parallel} by

$$\ddot{\xi} = \frac{q^*}{m^*} \mathbf{E}_{\parallel} =: q_0 \mathbf{E}_{\parallel}, \quad \mathbf{J} = n_{2D} q^* \dot{\xi} =: \sigma_0 \dot{\xi}, \quad \sigma = -n_{2D} q^* \nabla_{\parallel} \cdot \xi = -\sigma_0 \nabla_{\parallel} \cdot \xi,$$

n_{2D} being the two dimensional carrier density in the layer, and q^* and m^* being their charge and mass, respectively. Under these assumptions, the most general boundary conditions at the $i = 1, 2, 3 \dots$ -th boundaries are

$$\begin{aligned} \epsilon_i(\omega) f_i^z - \epsilon_{i-1}(\omega) f_{i-1}^z &= -\frac{\sigma_0 q_0}{\omega^2} \frac{\partial f_i^z}{\partial z}, \\ \frac{\partial f_i^z}{\partial z} - \frac{\partial f_{i-1}^z}{\partial z} &= 0, \quad \text{for the TM modes, and} \end{aligned} \tag{A1}$$

$$\begin{aligned} \frac{\partial g_i^z}{\partial z} - \frac{\partial g_{i-1}^z}{\partial z} &= \Omega g_i^z, \\ g_i^z - g_{i-1}^z &= 0, \quad \text{for the TE modes,} \end{aligned} \tag{A2}$$

with $\Omega = \mu_0 \sigma_0 q_0$. With these boundary conditions, the generating functions for the TM and TE modes, respectively, can be written in terms of the auxiliary functions

$$\begin{aligned} R_{\text{TM}}^{i,j} &= \frac{\epsilon_j(i\zeta_l) K_i - \epsilon_i(i\zeta_l) K_j - 2 \frac{\Omega}{\zeta_l^2} K_i K_j}{\epsilon_j(i\zeta_l) K_i + \epsilon_i(i\zeta_l) K_j + 2 \frac{\Omega}{\zeta_l^2} K_i K_j}, & R_{\text{TE}}^{i,j} &= \frac{K_i - K_j + 2\Omega}{K_i + K_j + 2\Omega} \\ S_{\text{TM}}^{i,j} &= \frac{\epsilon_j(i\zeta_l) K_i - \epsilon_i(i\zeta_l) K_j + 2 \frac{\Omega}{\zeta_l^2} K_i K_j}{\epsilon_j(i\zeta_l) K_i + \epsilon_i(i\zeta_l) K_j + 2 \frac{\Omega}{\zeta_l^2} K_i K_j}, & S_{\text{TE}}^{i,j} &= \frac{K_i - K_j - 2\Omega}{K_i + K_j + 2\Omega} \\ T_{\text{TM}}^{i,j} &= \frac{\epsilon_j(i\zeta_l) K_i + \epsilon_i(i\zeta_l) K_j - 2 \frac{\Omega}{\zeta_l^2} K_i K_j}{\epsilon_j(i\zeta_l) K_i + \epsilon_i(i\zeta_l) K_j + 2 \frac{\Omega}{\zeta_l^2} K_i K_j}, & T_{\text{TE}}^{i,j} &= \frac{K_i + K_j - 2\Omega}{K_i + K_j + 2\Omega} \end{aligned}$$

with $K_i = \sqrt{k_{\perp}^2 + \epsilon_i(i\zeta_l)\zeta_l^2}$, and $k_{\perp} = (k_x, k_y)$. Standard dielectric boundary conditions (dbc) are recovered by imposing $\Omega = 0$ and the plasma sheet boundary conditions (psbc) by requiring $\epsilon_j(i\zeta_l) = 1, \forall j$ (in this case $K_i = K_j$).

$$E^{ijk} = e^{-2d_j K_j} S^{j,k} R^{i,j} + 1,$$

$$\begin{aligned}
 F^{ijk} &= e^{-2d_j K_j} \mathbf{R}^{i,j} \mathbf{T}^{j,k} + \mathbf{R}^{j,k}, \\
 G^{ijk} &= e^{-2d_j K_j} \mathbf{S}^{j,k} \mathbf{T}^{i,j} + \mathbf{S}^{i,j}, \\
 H^{ijk} &= \mathbf{S}^{i,j} \mathbf{R}^{j,k} + e^{-2d_j K_j} \mathbf{T}^{i,j} \mathbf{T}^{j,k}.
 \end{aligned}$$

Considering henceforth all the cavities to be equal, we consider only the indices $\{ijk\} = \{012\}$, so that

$$\begin{aligned}
 I_1 &= E^{012}; \quad I_2 = F^{012} e^{-2d_2 K_2} G^{012}, \\
 I_n &= F^{012} e^{-2d_2 K_2} \left(H^{012} e^{-2d_2 K_2} \right)^{n-2} G^{012}, \quad \text{for } n \geq 3.
 \end{aligned}$$

Let us consider, for the case of the TM modes, three cavities. Letting $x_i = \sum_{n=0}^i d_n$, the matching conditions give rise to the 12×12 matrix of coefficients

$$M = \begin{pmatrix} -e^{-x_0 K_0} \epsilon_0 & -e^{-x_0 K_1} \epsilon_1 & e^{x_0 K_1} \epsilon_1 & 0 & 0 & 0 & 0 & 0 & 0 & 0 & 0 & 0 \\ -e^{-x_0 K_0} K_0 & e^{-x_0 K_1} K_1 & -e^{x_0 K_1} K_1 & 0 & 0 & 0 & 0 & 0 & 0 & 0 & 0 & 0 \\ 0 & e^{x_1 K_1} \epsilon_1 & e^{-x_1 K_1} \epsilon_1 & -e^{-x_1 K_2} \epsilon_2 & -e^{x_1 K_2} \epsilon_2 & 0 & 0 & 0 & 0 & 0 & 0 & 0 \\ 0 & e^{x_1 K_1} K_1 & -e^{-x_1 K_1} K_1 & e^{-x_1 K_2} K_2 & -e^{x_1 K_2} K_2 & 0 & 0 & 0 & 0 & 0 & 0 & 0 \\ 0 & 0 & 0 & e^{-K_2 x_2} \epsilon_2 & e^{K_2 x_2} \epsilon_2 & -e^{K_3 x_2} \epsilon_3 & -e^{-K_3 x_2} \epsilon_3 & 0 & 0 & 0 & 0 & 0 \\ 0 & 0 & 0 & -e^{-K_2 x_2} K_2 & e^{K_2 x_2} K_2 & -e^{K_3 x_2} K_3 & e^{-K_3 x_2} K_3 & 0 & 0 & 0 & 0 & 0 \\ 0 & 0 & 0 & 0 & 0 & e^{K_3 x_3} \epsilon_3 & e^{-K_3 x_3} \epsilon_3 & -e^{-K_4 x_3} \epsilon_4 & -e^{K_4 x_3} \epsilon_4 & 0 & 0 & 0 \\ 0 & 0 & 0 & 0 & 0 & e^{K_3 x_3} K_3 & -e^{-K_3 x_3} K_3 & e^{-K_4 x_3} K_4 & -e^{K_4 x_3} K_4 & 0 & 0 & 0 \\ 0 & 0 & 0 & 0 & 0 & 0 & 0 & e^{-K_4 x_4} \epsilon_4 & e^{K_4 x_4} \epsilon_4 & -e^{K_5 x_4} \epsilon_5 & -e^{-K_5 x_4} \epsilon_5 & 0 \\ 0 & 0 & 0 & 0 & 0 & 0 & 0 & -e^{-K_4 x_4} K_4 & e^{K_4 x_4} K_4 & -e^{K_5 x_4} K_5 & e^{-K_5 x_4} K_5 & 0 \\ 0 & 0 & 0 & 0 & 0 & 0 & 0 & 0 & 0 & e^{K_5 x_5} \epsilon_5 & e^{-K_5 x_5} \epsilon_5 & -e^{-K_6 x_5} \epsilon_6 \\ 0 & 0 & 0 & 0 & 0 & 0 & 0 & 0 & 0 & e^{K_5 x_5} K_5 & -e^{-K_5 x_5} K_5 & e^{-K_6 x_5} K_6 \end{pmatrix}$$

Computing the determinant of the minors of dimensions 4, 8, and 12, we obtain the energy of one, two, and three cavities, respectively. After regularization, for the single cavity (012) in Fig. 1, we find

$$\Delta_1 = E^{012} = I_1. \tag{A3}$$

For two cavities (012 – 234), we find

$$\begin{aligned}
 \Delta_2 &= E^{012} E^{234} + e^{-2(d_2 k_2)} F^{012} G^{234} =: (I_1)^2 + I_2, \text{ and} \\
 \log \Delta_2 &= \log(I_1^2) + \log\left(1 + \frac{I_2}{I_1^2}\right).
 \end{aligned} \tag{A4}$$

Finally, for the three cavities, we find

$$\begin{aligned}
 \Delta_3 &= E^{012} E^{234} E^{456} + e^{-2(d_2 k_2 + d_4 k_4)} F^{012} H^{234} G^{456} \\
 &\quad + e^{-2d_2 k_2} E^{456} F^{012} G^{234} + e^{-2d_4 k_4} E^{012} F^{234} G^{456} \\
 &=: I_1^3 + I_3 + I_1 I_2 + I_1 I_2, \\
 \log \Delta_3 &= \log(I_1^3) + \log\left(1 + \frac{2I_1 I_2}{I_1^3}\right) + \log\left(1 + \frac{I_3}{I_1^3 + 2I_1 I_2}\right).
 \end{aligned} \tag{A5}$$

$$\tag{A6}$$

When $d_2 \rightarrow \infty, I_2 \rightarrow 0$ and

$$\log \Delta_2 = \log I_1^2 = 2 \log I_1.$$

Thus, when the two cavities are far away, their energy is simply the sum of the individual contributions and $I^{(2)}$ can be seen as the energy due to the coupling of the two cavities (012)–(234). For the three cavities (012–234–456), the formulas are written so as to make evident the contribution to the energy resulting from the sum of the energies of the single cavities, with respect to the one coming from the coupling of the two possible pairs of cavities (012–234), (234–456), and the one coming from the coupling of the three, $I^{(3)}$.

References

1. E. Calloni, M. De Laurentis, R. De Rosa, F. Garufi, L. Rosa, L. Di Fiore, G. Esposito, C. Rovelli, P. Ruggi, F. Tafuri, Phys. Rev. D **90**(2), 022002 (2014)
2. G. Bimonte, E. Calloni, G. Esposito, L. Rosa, Phys. Rev. D **74** (2006) 085011 Erratum: Phys. Rev. D **75** (2007) 049904 Erratum: Phys. Rev. D **75**, 089901 Erratum: Phys. Rev. D **77**(2008), 109903 (2007)
3. S.A. Fulling, K.A. Milton, P. Parashar, A. Romeo, K.V. Shajesh, J. Wagner, Phys. Rev. D **76**, 025004 (2007)

4. G. Bimonte, G. Esposito, L. Rosa, *Phys. Rev. D* **78**, 024010 (2008)
5. G. Esposito, G.M. Napolitano, L. Rosa, *Phys. Rev. D* **77**, 105011 (2008)
6. H.B.G. Casimir, *Physica* **19**, 846 (1953)
7. L. Rosa et al., *Eur. Phys. J. Plus* **132**, 478 (2017)
8. A. Kempf, *J. Phys. A* **41**, 164038 (2008)
9. K.A. Milton, *The Casimir Effect* (World Scientific, Singapore, 2001)
10. M. Bordag, G.L. Klimchitskaya, U. Mohideen, V.M. Mostepanenko, *Advances in the Casimir Effect* (Oxford University Press, Oxford, 2009)
11. M. Bordag, U. Mohideen, V.M. Mostepanenko, *Phys. Rep.* **353**, 1 (2001)
12. J.D. Jackson, *Classical Electrodynamics* (Wiley, New York, 1998)
13. G. Barton, *J. Phys. A* **38**, 2997 (2005)
14. M. Bordag, I.G. Pirozhenko, V.V. Nesterenko, *J. Phys. A* **38**, 11027 (2005)
15. M. Bordag, *J. Phys. A* **39**, 6173 (2006)
16. M.T.D. Orlando, A.N. Rouver, J.R. Rocha, A.S. Cavichini, *Phys. Lett. A* **382**, 1486 (2018)
17. J. Silvester, *Math. Gazette Math. Assoc.* **84**(501), 460–467 (2000). <https://doi.org/10.2307/3620776>
18. D. Philip, Powell. [arXiv:1112.4379](https://arxiv.org/abs/1112.4379) [math.RA] (2011)
19. D.R. Harshman, A.P. Mills Jr., *Phys. Rev. B* **45**(18), 10684 (1992)
20. E. Tralbaldo, S. Ruffieux, E. Andersson, R. Arpaia, D. Montemurro, J.F. Schneiderman, A. Kalaboukhov, D. Winkler, F. Lombardi, T. Bauch, *Appl. Phys. Lett.* **116**, 132601 (2020)
21. E. Tralbaldo, C. Pfeiffer, E. Andersson, M. Chukharkin, R. Arpaia, D. Montemurro, A. Kalaboukhov, D. Winkler, F. Lombardi, T. Bauch, *IEEE Trans. Appl. Superconduct.* **30**(7), 1600904 (2020)
22. C.P. Poole Jr., A.H. Farach, J. Richard, Creswick, R. Prozorov, *Superconductivity* (Elsevier, Amsterdam, 2007)
23. Vilius Palenskis, *World J. Condens. Matter Phys.* **5**, 118 (2015)
24. Clément. Collignon, Benoit Fauqué, Antonella Cavanna, Ulf Gennser, Dominique Mailly, Kamran Behnia, *Phys. Rev. B* **94**, 224506 (2017)